Y.-W. Lin, S. Lee, Z. Ren, and C. T.-C. Nguyen, "Series-resonant micromechanical resonator oscillator," *Technical Digest*, 2003 IEEE International Electron Devices Meeting, Washington, DC, Dec. 8-10, 2003, pp. 961-964.

Series-Resonant Micromechanical Resonator Oscillator

Yu-Wei Lin, Seungbae Lee, Zeying Ren, and Clark T.-C. Nguyen

Center for Wireless Integrated Microsystems
Department of Electrical Engineering and Computer Science
University of Michigan, Ann Arbor, Michigan 48109-2122 USA
TEL: (734)764-3352, FAX: (734)647-1781, email: ywlin@umich.edu

ABSTRACT

A 10-MHz series resonant micromechanical resonator oscillator has been demonstrated using a custom-designed, single-stage, zero-phase-shift sustaining amplifier together with a clamped-clamped beam micromechanical resonator, designed with a relatively large width of 40 µm to achieve substantially lower series motional resistance R_x and higher power handling than previous such devices. Using automatic level control (ALC) circuitry to remove an unexpected $1/f^3$ close-to-carrier phase noise component, this oscillator achieves a phase noise density of −95 dBc/Hz at 1 kHz offset from the carrier, while consuming only 820 µW of power.

I. INTRODUCTION

Recent interest in ultra-thin (credit card) wireless devices have fueled efforts to flatten the form factors of the off-chip passives needed for filtering and frequency generation in wireless communication circuits. Among functions requiring passives, the quartz crystal reference oscillator is one of the most difficult to miniaturize, since the Q >10,000 and thermal stability better than 35 ppm over 0-70°C of its off-chip quartz crystal tank constitute relatively severe specifications. Nevertheless, an on-chip vibrating clamped-clamped beam ("CC-beam") micromechanical resonator based on MEMS technology has been demonstrated at 10 MHz with a Q of 4,000 and a frequency stability of 34 ppm over 0-70°C [1], which matches that of quartz, and which provides a potential path towards a fully integrated communications reference oscillator.

This paper approaches such integration levels by demonstrating a 10-MHz series resonant oscillator using a custom-designed, single-stage, zero-phase-shift sustaining amplifier IC together with a CC-beam micromechanical resonator, designed with a relatively large width of 40 µm to achieve substantially lower series motional resistance R_x and higher power handling than previous such devices. Although widening of the resonator beam lowers its R_x, and thereby allows the use of a lower noise, lower power single-stage sustaining amplifier, it also seems to lower the resonator's Q from the ~3,000 normally seen for 8-µm wide devices [2], to only 1,036. Nevertheless, this Q is still more than two orders of magnitude larger than achievable by an on-chip inductor-capacitor pair, and the oscillator demonstrated here still achieves a phase noise of −95 dBc/Hz at 1 kHz offset from the carrier, while consuming only 820 µW of power, which is substantially lower than the mW's typically needed by the quartz crystal oscillators presently used in cellular telephones. This, together with its potential for full integration of the transistor sustaining circuit and MEMS device onto a single silicon chip, makes the microechanical resonator oscillator of this work an attractive on-chip replacement for quartz crystal reference oscillators in communications and other applications.

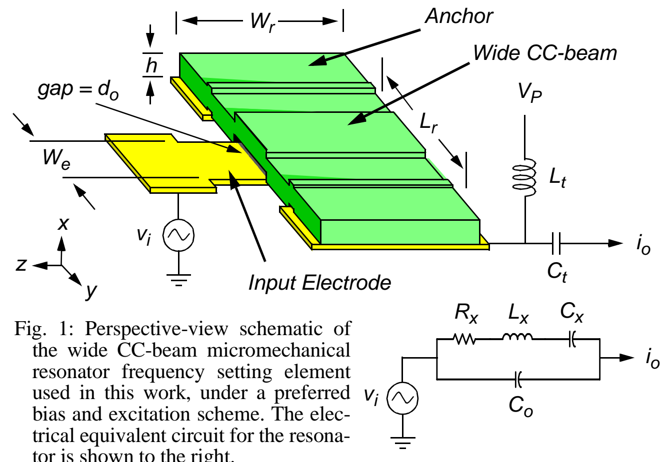

Fig. 1: Perspective-view schematic of the wide CC-beam micromechanical resonator frequency setting element used in this work, under a preferred bias and excitation scheme. The electrical equivalent circuit for the resonator is shown to the right.

II. MICROMECHANICAL RESONATOR DESIGN

The four resonator attributes that most influence oscillator design and performance are its Q, resonance frequency, series motional resistance, and power handling ability. In general, these parameters are strong functions of both the resonator geometry and the bias and excitation signals applied to it.

Figure 1 presents a perspective-view schematic of the wide CC-beam resonator used in this work, together with a one-port bias and excitation scheme, and an equivalent electrical model. To excite the CC-beam, a dc-bias V_P is applied to conductive beam, and an ac voltage v_i applied to its electrode. This voltage combination generates a time-varying force that drives the beam into mechanical vibration when the frequency of v_i matches the beam resonance frequency f_o, given by [3]

$$f_o = 1.03\kappa\sqrt{\frac{E}{\rho}}\cdot\frac{h}{L_r^2}\cdot\left[1-\left(\frac{k_e}{k_m}\right)\right]^{1/2} \quad (1)$$

where E and ρ are the Young's modulus and density, respectively, of the structural material; h and L_r are specified in Fig. 1; k_m and k_e are the purely mechanical and the electrical spring constants, respectively; and κ is a scaling factor that models the effect of surface topography.

The ensuing resonance vibration creates a dc-biased (by V_P) time-varying capacitance between the beam and its underlying electrode through which a current equal to

$$i_o = V_P\cdot\frac{\partial C}{\partial x}\cdot\frac{\partial x}{\partial t} = V_P\cdot\left(\frac{\varepsilon_o W_r W_e}{d_o^2}\right)\cdot(\omega_o X) \quad (2)$$

can be sensed as the output of this device, where X is the

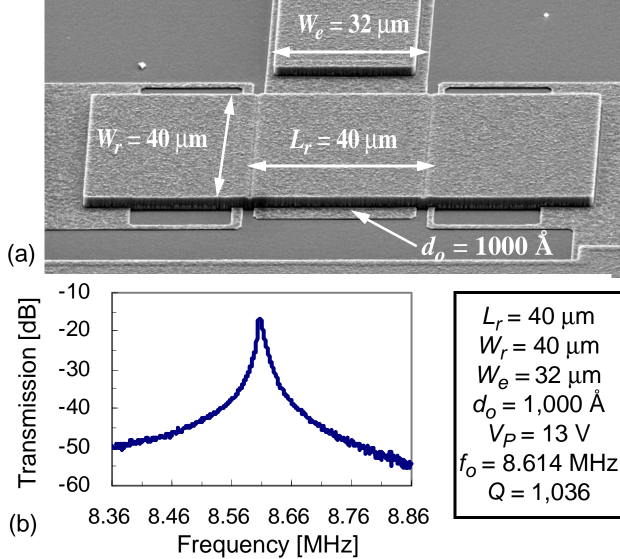

Fig. 2: (a) SEM and (b) measured frequency characteristic for a fabricated CC-beam micromechanical resonator, featuring large beam and electrode widths for lower R_x and higher power handling ability.

amplitude of vibration, and ω_o is the radian resonance frequency, and other variables are specified in Fig. 1. The CC-beam resonator of this work generates its maximum output when its vibration amplitude reaches a maximum acceptable value $X_{max}=ad_o$, which is set either by automatic level control (ALC), or by the pull-in limit (for which a=0.56 at resonance). Using (2), the maximum power P_{omax} that this device can handle can then be expressed by

$$P_{omax} = \frac{\omega_o}{Q} k_r a^2 d_o^2 \tag{3}$$

where $k_r = k_m - k_e$. Equation (3) asserts that higher power handling can be attained with larger values of stiffness k_r and electrode-to-resonator gap spacing d_o.

The series motional resistance R_x of the resonator governs the relationship between v_i and i_o and is determined approximately by the expression

$$R_x = \frac{v_i}{i_o} = \frac{k_r}{\omega_o Q V_P^2} \cdot \frac{d_o^4}{\varepsilon_o^2 W_r^2 W_e^2} \tag{4}$$

where k_r is the lumped stiffness of the beam at its center. Equation (1) predicts that an increase in beam width W_r leads to a smaller R_x, and this, together with increasing the electrode width W_e to further increase transducer capacitance, comprises the basic strategy used in this work to achieve an R_x small enough to allow the use of a single-stage sustaining amplifier.

Unfortunately, increasing W_r also seems to lower the Q and increase the k_r of the CC-beam, and according to (4), this reduces the degree to which R_x is lowered. To illustrate, Fig. 2 presents the SEM and measured frequency characteristic (under vacuum) for a 40µm-wide, 32µm-wide-electrode 10-MHz CC-µbeam, showing a Q of 1,036, which is 3X lower than exhibited by previous 8µm-wide beams. This reduction in Q with increasing beam width is believed to arise from increased energy loss through the anchors to the substrate, caused by increases in CC-beam stiffness and in the size of its anchors. Figure 3(a) and (b)

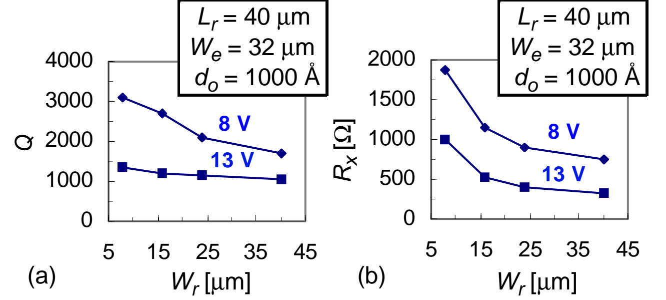

Fig. 3: Measured plots of (a) Q; and (b) series motional resistance R_x, versus beam width W_r for V_P = 8 V and 13 V, showing a net decrease in R_x, despite a decrease in Q.

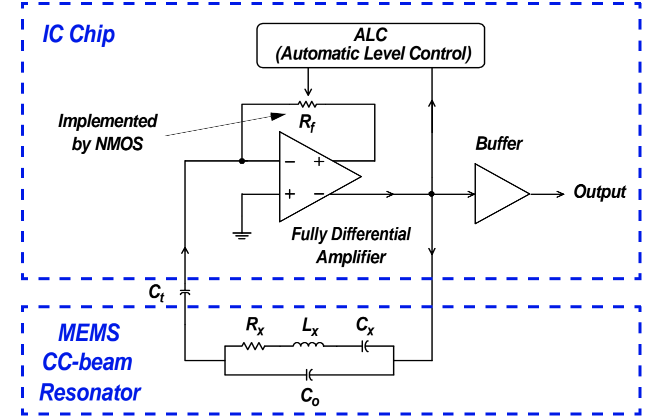

Fig. 4: Top-level circuit schematic of the micromechanical resonator oscillator of this work. Here, the micromechanical resonator is represented by its equivalent electrical circuit.

present plots of Q and R_x versus beam width W_r, showing that despite reductions in Q, the net effect of beam-widening is still a decrease in R_x. In particular, beam-widening has reduced the R_x of a clamped-clamped beam resonator from the 17 kΩ of previous work [2], to now only 340 Ω

In addition to a lower R_x, and perhaps more importantly, the use of a larger CC-beam width provides the additional advantage of a larger power handling ability, which comes about due to increased stiffness k_r. In particular, the stiffness of the 40µm-wide beam used here is 12,000 kg/m^3, which is 8X larger than the 1,500 kg/m^3 of an 8µm-wide predecessor [2], which (accounting for decreased Q) according to (3), provides a net 2.67X higher oscillator output power. For the same V_P, this should result in a 4.27 dB lower far-from-carrier phase noise floor.

III. OSCILLATOR CIRCUIT DESIGN

Fig. 4 presents the top-level schematic of the oscillator circuit used here, where the CC-beam is represented by its equivalent *LCR* circuit. As shown, a series resonant configuration is used, employing a transresistance sustaining amplifier in order to better accommodate the medium-range resistance of the CC-beam frequency-setting element. The conditions required for sustained oscillation can be stated as follows:

(1) The total phase shift around the closed positive feedback loop must be 0°. In this series resonant topology, both the resonator and sustaining amplifier have 0° phase shifts from input to output.

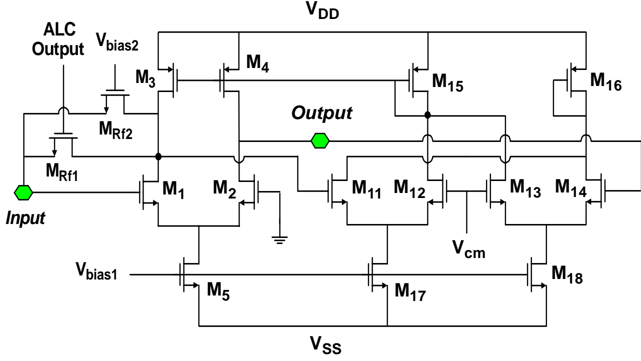

Fig. 5: Detailed circuit schematic of the single-stage sustaining transresistance amplifier of this work, implemented by a fully-differential amplifier in a shunt-shunt feedback configuration.

(2) The gain of the transresistance sustaining amplifier R_{amp} should be larger than the sum of the μmechanical resonator's motional resistance, plus the input and output resistances of the sustaining amplifier; i.e.,

$$R_{amp} \geq R_x + R_i + R_o \tag{5}$$

The use of a resonator with an R_x more than 60X lower than achieved by previous CC-beams [2] greatly reduces the gain R_{amp} required for oscillation start-up, to the point where a single-stage (rather than two-stage) transresistance sustaining amplifier, shown in Fig. 5, can now achieve sufficient gain to instigate oscillation. The use of a single-stage gain circuit provides not only power consumption and complexity advantages, but as indicated in [4], also offers noise advantages over two-stage counterparts.

The particular sustaining amplifier circuit of Fig. 5 differs from previous two-stage circuits [2][4] not only in the number of stages used, but in that it achieves the needed 0° phase shift for oscillation in only a single stage, which improves both its noise and bandwidth performance. As shown in the coarse oscillator schematic of Fig. 4, the sustaining circuit is composed of a fully balanced differential CMOS op amp hooked in shunt-shunt feedback on one side, with the output taken from the other. By taking the output from the other side of the differential op amp, an additional 180° phase shift is added on top of the 180° shift from the shunt-shunt feedback, resulting in a total 0° phase shift from input to output, while preserving a low output resistance (due to symmetry) obtained via shunt-shunt feedback. In the detailed circuit schematic of Fig. 5, transistors M_1-M_5 comprise the basic differential op amp, while M_{11}-M_{18} constitute a common-mode feedback circuit that sets its bias point. The MOS resistors M_{Rf1} and M_{Rf2} serve as a shunt-shunt feedback elements that allow control of the transresistance gain via adjustment of their gate voltages.

In addition to the base sustaining amplifier, the oscillator IC also includes an automatic level control (ALC) circuit, shown in Fig. 6. This circuit consists of an envelope detector that effectively measures the oscillation amplitude, followed by a comparator that feeds back to the gain-setting MOS resistor M_{Rf1} to match the oscillation amplitude to a preset reference level applied to the negative input of the comparator. As shown in [5], ALC has proven effective in removing the $1/f^3$ close-to-carrier phase noise that has plagued previous off-chip micromechanical resonator oscillators.

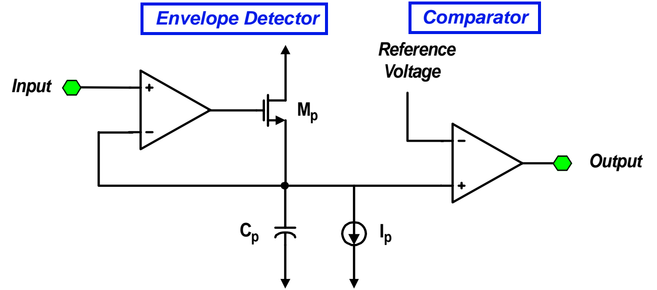

Fig. 6: Top-level circuit schematic of the automatic level control circuit.

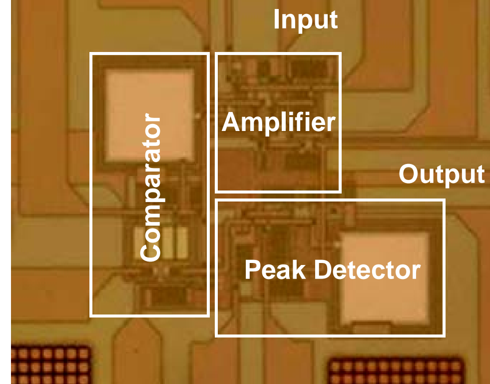

Fig. 7: Photo of the sustaining transresistance amplifier IC fabricated in TSMC's 0.35 μm CMOS process.

Table 1: Oscillator Design Summary

Integrated Circuit	Process	TSMC 0.35 μm
	Voltage Supply	± 1.65 V
	Amplifier Gain	2 kΩ
	Amplifier BW	75 MHz
	Power Cons. (Amp)	400 μW
	Power Cons. (ALC)	430 μW
	Area	140 μm × 100 μm
CC-Beam μMechanical Resonator	Process	All-Polysilicon Surface Micromaching
	L_r, W_r, W_e	40, 40, 32 μm
	d_o	1000 Å
	DC Bias Voltage	13 V
	Power Consumption	~ 0 W
	Area	100 μm × 60 μm

IV. EXPERIMENTAL RESULTS

Micromechanical CC-beams were fabricated using a small-vertical gap polysilicon surface-micromachining process previously used to achieve HF mixer-filter devices [6]. Fig. 2 already presented the SEM for the CC-beam of this work. Figure 7 presents a photo of the amplifier IC, which was fabricated in TSMC's 0.35 μm process. The IC chip area is about 140μm×100μm, which together with the 100μm×60μm required for the CC-beam, yields the smallest footprint to date for a high-Q reference oscillator at 10 MHz. Table 1 summarizes the design of the overall oscillator circuit.

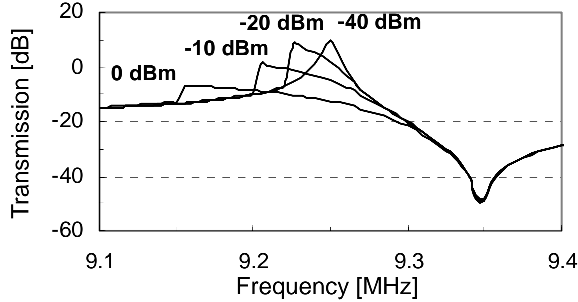

Fig. 8: Measured open-loop gain of the oscillator circuit under increasing input signal amplitudes.

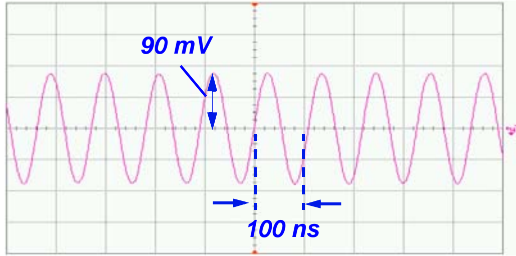

Fig. 9: Measured oscilloscope waveform of the micromechanical resonator oscillator of Fig. 4 in steady-state.

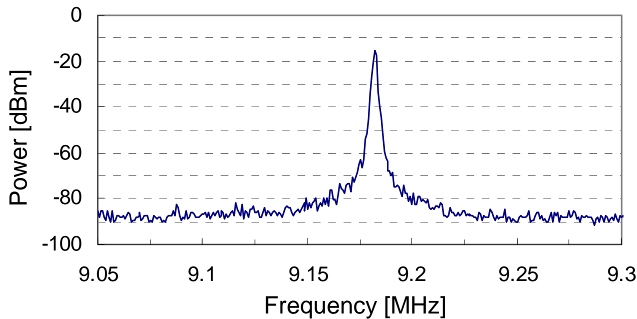

Fig. 10: Fourier spectrum as measured by a spectrum analyzer of the micromechanical resonator oscillator output waveform.

Interconnections between the IC and MEMS chips were made via wire-bonding, and testing was done under vacuum to preserve the high Q of the micromechanical resonator. Figure 8 presents the measured open-loop gain of the oscillator at various input power levels, showing a spring-softening Duffing nonlinearity that likely contributes to limiting of the oscillation amplitude when the ALC is not engaged. Figures 9-11 present oscillator performance data, starting with the obligatory oscilloscope and spectrum analyzer waveforms, and culminating in a plot of phase noise density versus offset from the carrier frequency. The last of these shows a phase noise of −80 dBc/Hz at 1 kHz offset from the carrier, dropping to −120 dBc/Hz at far-from-carrier offsets, with the ALC disengaged. This far-from-carrier noise floor is 15 dB better than that of an oscillator using an 8μm-wide CC-beam resonator [5], verifying the utility of wide CC-beam design. However, the close-to-carrier noise performance is somewhat poor due to a $1/f^3$ dependence that most likely derives from the Duffing-based limiting of this oscillator. With ALC engaged, this $1/f^3$ noise component is removed, leaving an expected $1/f^2$ close-to-carrier component commonly exhibited by high Q oscillators, and allowing a much-improved phase noise density of −95 dBc/Hz at 1 kHz offset. Due to the smaller power level of the oscillator when ALC is engaged, the far-from-carrier phase noise density increased a bit to −110 dBc/Hz. It is expected that this problem should be solvable in the future by replacing the CC-beam with a recently demonstrated wine-glass disk resonator, which sports higher Q and higher power handling [7].

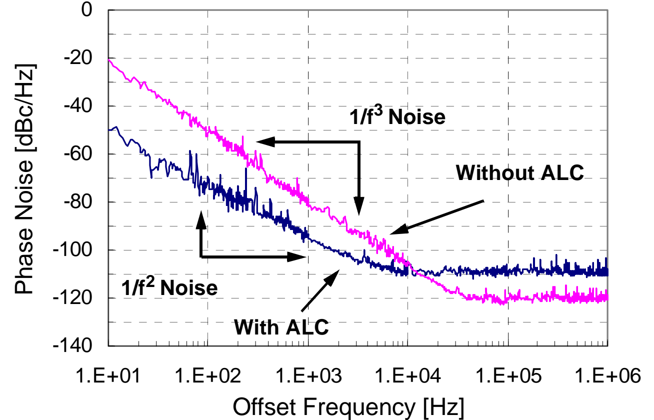

Fig. 11: Phase noise density versus carrier offset frequency plot for the micromechanical resonator oscillator of Fig. 4, measured by an HP E5500 Phase Noise Measurement System.

V. CONCLUSIONS

A 10-MHz series resonant oscillator has been demonstrated using only on-chip components, including a custom-designed, single-stage, zero-phase-shift sustaining amplifier IC together with a large-width CC-beam micromechanical resonator. The phase noise performance of this oscillator is on par with that of low-end crystal oscillators when ALC is employed to eliminate a $1/f^3$ close-to-carrier noise component. Further performance improvements towards cellular phone specifications can be expected if the power handling and Q of the frequency-setting micromechanical resonator can be improved. In this regard, recently demonstrated wine-glass mode disk resonators, with Q's ~98,000 at 73 MHz, may fit the bill for future communications-grade reference oscillators.

Acknowledgement: This work was supported by DARPA Grant No. F30602-01-1-0573.

References:

[1] W.-T. Hsu and C. T.-C. Nguyen, "Stiffness-compensated temperature-insensitive micromechanical resonators," MEMS'02, pp. 731-734.

[2] S. Lee and C. T.-C. Nguyen, "A 10-MHz micromechanical resonator Pierce oscillator for communications," Transducers'01, pp. 1094-1097, June, 2001.

[3] F. D. Bannon III, J. R. Clark, and C. T.-C. Nguyen, "High-Q HF microelectromechanical Filters," *IEEE J. Solid-State Circuits*, Vol. 35, no. 4, pp. 512-526, Apr. 2000.

[4] C. T.-C. Nguyen and R. T. Howe, "An integrated CMOS micromechanical resonator high-Q oscillator," *IEEE J. Solid-State Circuits*, vol. 34, no. 4, pp. 440-455, April 1999.

[5] S. Lee and C. T.-C. Nguyen, "Influence of automatic level control on micromechanical resonator oscillator phase noise," to be published in the *Proceedings*, Frequency Control Symposium'03, May 5-8, 2003.

[6] A.-C. Wong, H. Ding, and C. T.-C. Nguyen, "Micromechanical mixer+filters," IEDM'98, Dec. 8-10, 1998, pp. 471-474.

[7] M. A. Abdelmoneum, M. U. Demirci, and C. T.-C. Nguyen, "Stemless wine-glass-mode disk micromechanical resonators," MEMS'03, Jan. 19-23, 2003, pp. 698-701.